Evaluation of Long Range GNSS Ambiguity Resolution

P.J.G. Teunissen, P. Joosten and N.F. Jonkman

Department of Mathematical Geodesy and Positioning
Faculty of Civil Engineering and Geosciences
Delft University of Technology
The Netherlands

BIOGRAPHY

Dr. Peter Teunissen is Professor of Mathematical Geodesy and Positioning at the Delft University of Technology. Peter Joosten and Niels Jonkman both graduated at the Department of Mathematical Geodesy and Positioning of the University. They are currently engaged in the development of GNSS data processing strategies for medium scaled networks with an emphasis on ambiguity resolution.

ABSTRACT

In developing new (Galileo) or modernized (GPS) Global Navigation Satellite Systems (GNSS), several design parameters are distinguished that contribute to fast carrier phase ambiguity resolution, and thus also to precise positioning in (near) real-time. Ambiguity resolution can amongst others be influenced by varying the precision of the observables and the number and spacing of the navigation frequencies.

In this study, the ambiguity resolution success rate, being the probability of estimating ambiguities at their correct integer values, will be defined and discussed. As will be demonstrated, the success-rate can serve as a design tool to infer the value of the system design parameters for ambiguity resolution.

1. INTRODUCTION

In the daily practice of GNSS ambiguity resolution, the resolved integer ambiguities are usually treated as deterministic variates. Strictly speaking this is incorrect, since the resolved ambiguities are functions of the stochastic data and therefore stochastic variates as well. Hence, a prerequisite for treating the resolved ambiguities deterministically, is that one verifies whether or not the probability mass function of the estimated integer ambiguities is sufficiently peaked. In particular one should verify explicitly whether the probability of correct integer estimation, the success rate, is sufficiently close to one. One can not expect to have a reliable ambiguity resolution when this probability differs too much from one.

In this contribution, the expected performance of long range ambiguity resolution based on the geometry-free GNSS model is analyzed. The ambiguity success rate of the LAMBDA method is used to measure this performance. The dependence of the success rate on the number and spacing of the navigation frequencies is particularly emphasized.

2. THE LAMBDA METHOD

2.1 The observation equations

The GNSS models on which ambiguity resolution is based, can all be cast in the following conceptual frame of linear(ized) observation equations

$$y = Aa + Bb + e \qquad (2.1)$$

where y is the given GNSS data vector, a and b are the unknown parameter vectors of order n and o respectively, and where e is the noise vector of order m. The matrices A and B are the corresponding design matrices of order $m \times n$ and $m \times o$ respectively. The data vector y will usually consist of the 'observed minus computed' single- or dual-frequency double-differenced (DD) phase and/or pseudo range (code) observations, accumulated over all observation epochs. The entries of vector a are then the DD carrier phase ambiguities, expressed in units of cycles rather than range. They are known to be integers. The entries of vector b will consist of the remaining unknown parameters, such as for instance baseline components (coordinates) and possibly atmospheric delay parameters (troposphere, ionosphere).

The procedure which is usually followed for solving the above model can be divided into three steps [for more details we refer to e.g. *Teunissen* (1993), *de Jonge and Tiberius* (1996), or to the textbooks *Hofmann-Wellenhof et al.* (1997), *Strang and Borre* (1997) and *Teunissen and Kleusberg* (1998)]:

- In the *first* step one simply disregards the integer constraints on the ambiguities and performs a standard adjustment. As a result one obtains the (real-valued) least-squares estimates of a and b, together with their variance-covariance (vc-) matrix

$$\begin{bmatrix} \hat{a} \\ \hat{b} \end{bmatrix}; \begin{bmatrix} Q_{\hat{a}} & Q_{\hat{a}\hat{b}} \\ Q_{\hat{b}\hat{a}} & Q_{\hat{b}} \end{bmatrix} \tag{2.2}$$

  This solution is often referred to as the 'float' solution.
- In the *second* step the 'float' ambiguity estimate $\hat{a}$ is used to compute the corresponding integer ambiguity estimate $\breve{a}$. This implies that a mapping $F: R^n \rightarrow Z^n$, from the n-dimensional space of reals to the n-dimensionsal space of integers, is introduced such that

$$\breve{a} = F(\hat{a}) \tag{2.3}$$

- Once the integer ambiguities are computed, they are used in the *third* step to finally correct the 'float' estimate of b. As a result one obtains the 'fixed' solution

$$\breve{b} = \hat{b} - Q_{\hat{b}\hat{a}} Q_{\hat{a}}^{-1} (\hat{a} - \breve{a}) \tag{2.4}$$

  This expression shows how the residual $(\hat{a} - \breve{a})$ is used to adjust the 'float' solution so as to obtain the final 'fixed' solution.

2.2 The precision of the solution

It is the purpose of ambiguity resolution to improve significantly upon the precision of the estimated parameters by means of the integer ambiguity constraints. This is the *essence* of ambiguity resolution. That is, ambiguity resolution only makes sense when the precision of the 'fixed' solution $\breve{b}$ is significantly better than that of the corresponding 'float' solution $\hat{b}$. In order to obtain the vc-matrix of the 'fixed' solution $\breve{b}$, one needs to apply the error propagation law to Eq. (2.4). While doing so, one needs to recognize that not only the real-valued vectors $\hat{a}$ and $\hat{b}$ are random, but the integer vector $\breve{a}$ as well. Hence, all three vectors will contribute to the vc-matrix of the 'fixed' solution. As shown in *Teunissen* (1998a) the resulting vc-matrix of Eq. (2.4) reads

$$Q_{\breve{b}} = \underbrace{Q_{\hat{b}} - Q_{\hat{b}\hat{a}} Q_{\hat{a}}^{-1} Q_{\hat{a}\hat{b}}}_{1} + \underbrace{Q_{\hat{b}\hat{a}} Q_{\hat{a}}^{-1} Q_{\breve{a}} Q_{\hat{a}}^{-1} Q_{\hat{a}\hat{b}}}_{2} \tag{2.5}$$

in which $Q_{\breve{a}}$ denotes the vc-matrix of the integer ambiguity estimator. The first term on the right hand side captures the contribution of $\hat{a}$ and $\hat{b}$, while the second term captures the contribution of $\breve{a}$. In practice, this second term is usually neglected. As a result the vc-matrix of the 'fixed' solution is approximated by the first term, which indeed is smaller than the vc-matrix of the original 'float' solution.

2.3 The ambiguity success rate

It will be clear that the first term of Eq. (2.5) only provides a good approximation to the vc-matrix of the 'fixed' solution, when $Q_{\breve{a}}$ is sufficiently small. For this to be the case the probability distribution of the integer ambiguity estimator needs to be sufficiently peaked. This distribution, which is a probability *mass* function, will be sufficiently peaked when the probability of correct integer estimation, the *success rate*, is sufficiently close to one. That is, when

$$P(\breve{a} = a) = 1 - \varepsilon \quad \text{with } \varepsilon \text{ small} \tag{2.6}$$

It is thus of importance that one is able to check whether Eq. (2.6) is valid or not. Only then will one be allowed to assume safely that the integer ambiguity estimator is sufficiently nonrandom. And only then can one expect the first term of Eq. (2.5) to give an adequate description of the precision characteristics of the 'fixed' solution.

The probability of correct integer ambiguity estimation depends on the probability distribution of $\hat{a}$ and on the chosen integer map $F: R^n \rightarrow Z^n$. We will assume that the 'float' solution is unbiased and normally (Gaussian) distributed. Thus

$$\hat{a} \sim N(a, Q_{\hat{a}}) \tag{2.7}$$

This will be the case when the zero mean noise vector e is normally distributed and the 'float' solution is obtained by means of a least-squares adjustment.

For the integer map $F: R^n \rightarrow Z^n$ of Eq. (2.3) one has a variety of options available. Every map which turns a real vector into an integer vector could be chosen in principle. In *Teunissen* (1998b) a whole class of *unbiased* integer ambiguity estimators is introduced. Members from this class are the ambiguity estimators that follow from 'integer rounding', 'integer bootstrapping' or 'integer least-squares'. From a computational point of view, 'integer rounding' provides the simplest estimator, while 'integer least-squares' is more complex.

2.4 Integer least-squares

Ambiguity resolution based on integer least-squares was first introduced in (*Teunissen*, 1993), and is made operational in the Least-squares AMBiguity Decorrelation Adjustment or LAMBDA-method. Although more complex than the simple integer rounding principle, integer least-squares has a superior performance in the sense that it maximizes the probability of estimating ambiguities at their correct integer values, (*Teunissen*, 1999). In other words, of all possible integer estimation techniques, integer least-squares will yield the highest possible ambiguity success rates. The probability mass function of the integer least-squares ambiguity estimator, and ways of

computing the corresponding ambiguity success rates, are given in *Teunissen* (1998c,d) and the references cited therein.

Starting point for the integer least-squares ambiguity estimation with the LAMBDA-method is an ordinary least-squares adjustment of the GNSS observations. The constraining of the resulting real-valued ambiguity estimates to integers can then be phrased in terms of the following minimization problem

$$\min_{a} (\hat{a}-a)^T Q_{\hat{a}}^{-1} (\hat{a}-a), \text{with } a \in Z^n \qquad (2.8)$$

This minimization problem defines the integer map $F: R^n \rightarrow Z^n$ of Eq. (2.3) implicitly. The integer least-squares solution $\breve{a}$ is the integer vector nearest to the float solution, where nearness is measured in the metric of the vc-matrix of the float solution. If this matrix were to be a diagonal matrix and the least-squares ambiguity estimates thus uncorrelated, the integer solution could be determined by a simple rounding of the entries of $\hat{a}$. For GNSS observations however, the estimates are usually highly correlated, and the integer solution has to be identified by a discrete search in a subspace of Z^n, the integer ambiguity search space.

The search for the solution of the integer least-squares minimization problem is hampered by the strong correlation and poor precision of the (real-valued) least-squares ambiguity estimates. To improve the computational efficiency of the discrete search, the LAMBDA method therefore employs a decorrelating Z-transformation. This Z-transformation manages to retain the integer character of the minimization problem whilst at the same time lowers the correlation and improves the precision of the transformed ambiguity estimates. The transformed search space allows a relatively easy identification of the integer least-squares solution, as it has a more sphere-like shape. For a detailed description of both the search and the construction of the Z-transformation, the reader is referred to (*de Jonge and Tiberius*, 1996).

Summarizing, the LAMBDA-method is applicable to any model in which integer parameters appear. The method produces an *optimal* integer ambiguity solution by means of *efficiently* solving the integer least-squares problem through the use of a *decorrelation* process. At present the method is already widely used for various single- and dual-frequency GPS processing applications. The method is however also applicable and suitable for a three (or more) carrier system. It is therefore applicable to the modernized GPS and to the Galileo system, without any modifications to the method at all, see (*Joosten et al.*,1999). In the remaining part of this contribution the method will be used to study the frequency dependence of the geometry-free ambiguity success rates. Previous studies on this subject can be found in amongst others (*Hatch*, 1996), (*Forsell et al.*,1997), (*Vollath et al.*, 1998), (*Ericson*, 1999) and (*Han and Rizos*, 1999).

3. THE GEOMETRY-FREE GNSS MODEL

The geometry-free model is the simplest possible mathematical model for the adjustment of GNSS observations that still allows the estimation of integer carrier phase ambiguities, see e.g. (*Hatch*, 1982), (*Euler and Goad*, 1990), (*Teunissen*, 1996). In its most basic form, the model consists of the DD pseudo range (code) and carrier phase observations of two receivers to two satellites, parametrized in terms of an unknown DD satellite-receiver range, unknown integer ambiguities and an unknown ionospheric delay

$$\begin{aligned} \phi_\alpha(i) &= \rho(i) - (\lambda_\alpha/\lambda_1)^2 I(i) + \lambda_\alpha a_\alpha \\ p_\alpha(i) &= \rho(i) + (\lambda_\alpha/\lambda_1)^2 I(i) \end{aligned} \qquad (3.1)$$

where ϕ and p indicate the carrier phase and pseudo range observations in units of range rather than cycles, ρ, a and I denote the unknown range, the integer phase ambiguity and the ionospheric delay, λ denotes the known wavelength of the carrier, i refers to the time epoch and α ranges from one to two, or from one to three, depending on whether a dual-frequency or triple-frequency system is used.

Note, due to the parametrization in terms of the DD ranges, that no linearization is required for the above observation equations. The absence of the receiver-satellite geometry also implies that the model permits both receivers to be either stationary or moving. Furthermore, the parametrization in terms of the DD ranges implies that the tropospheric delays need not be modelled explicitly. When present, these delays will get lumped with the DD ranges. Hence the estimated ambiguities will always be free from tropospheric biases.

In the following it will be assumed that the 'float' solution of the above model is obtained in a standard least-squares sense. The ambiguities are considered to be time-invariant for the duration of the observation period. We also assume that time correlation and cross correlation are absent. Unless otherwise stated, the *undifferenced* variances of the carrier phase and pseudo range (code) observations are chosen as $\sigma_\phi^2=(3mm)^2$ and $\sigma_p^2=(30cm)^2$.

3.1 Dual-frequency analysis

As a preparation for our analysis of the triple-frequency GNSS geometry-free model, we will first study the dual-frequency ambiguity success rate and its dependence on a varying second frequency $f_2=c/\lambda_2$, whilst the first frequency is kept fixed to the GPS L1 frequency. This is shown in figure 3-1. A number of remarks are in order. First note that the success rate fails to exceed the very small value of 0.025 within the frequency range of [1000(Mhz), 2000(Mhz)]. This stipulates the poor performance of *instantaneous* dual-frequency ambiguity resolution for long distances, distances for which the ionospheric delays are unknown

(ionosphere-float). In these cases one can not expect dual-frequency ambiguity resolution to be successful. The figure also shows that the success rate reaches its minimum when $f_2=f_1$ and that the success rate gets larger when the frequency separation gets larger. This contradicts the popular belief that ambiguity resolution would benefit from choosing frequencies close together. It is of course still true that frequencies with little separation would allow one to construct a wide-lane with a corresponding very large wavelength. However, as the figure shows this turns out to be counterproductive as far as the overall success rate is concerned. In fact, as the figure shows, the success rate will be identical to zero when the two frequencies coincide. This is understandable when one recognizes that a nonzero frequency separation is needed per se in order to be able to estimate the ionospheric delays. When the two frequencies coincide, the ionospheric delays become non-estimable and the vc-matrix of the ambiguities becomes singular. As a consequence, the success rate reduces to zero.

Finally note that the success rates are somewhat larger at the lower end of the spectrum than at the higher end of the spectrum. This effect is due to the assumed frequency independence of the measurement precision.

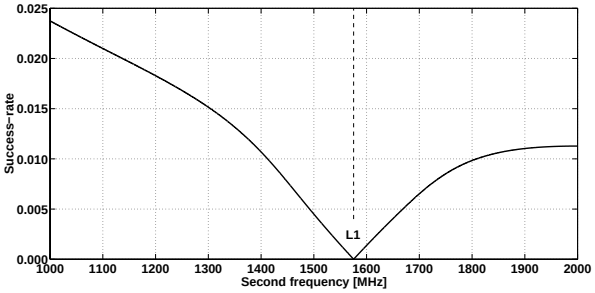

Figure 3-1: The single epoch, ionosphere-float, dual-frequency ambiguity success rate as function of the second frequency in MHz.

In the actual practice of GNSS there are still many who, for inferring the quality of ambiguity resolution, base their judgement on the precision of the ambiguities. That this approach should be avoided and that the success rate itself should be used as the quality indicator for ambiguity resolution, is made clear by figure 3-2. This figure shows the precision of the ambiguities. The top graph shows the standard deviations of the two DD ambiguities, while the lower graph shows the standard deviations of the two LAMBDA transformed ambiguities. The two graphs clearly differ. In the DD case the two curves (almost) coincide, while in the transformed case the two curves show a distinct difference. This emphasizes the fact that these standard deviations are dependent on the chosen ambiguity parametrization. Hence, they should not be used to judge the quality of ambiguity resolution. Only the least-squares success rate provides an objective measure, as it is independent of the chosen ambiguity parametrization.

In case the ambiguities would be uncorrelated, the signature of their precision curves can be used to *explain* the shape of the success rate curve. To a good approximation this also applies to the LAMBDA transformed ambiguities. Of the two transformed ambiguities, one is of excellent precision while the other is of poor precision. Since these two ambiguities are (almost) decorrelated, the signature of the precision curve of the poorly determined ambiguity will dominate the shape of the success rate curve. Compare figure 3-2 with figure 3-1.

Finally note from a comparison of the two graphs of figure 3-2 that although the ambiguity vc-matrix is singular in case the two frequencies coincide, there still exists an estimable integer ambiguity. Although the standard deviations of the two DD ambiguities are both infinite in this case, the standard deviation of one of the two transformed ambiguities is still very small. This is due to the fact that the difference of the two DD ambiguities can still be estimated very precisely from the phase data, in case the two frequencies coincide.

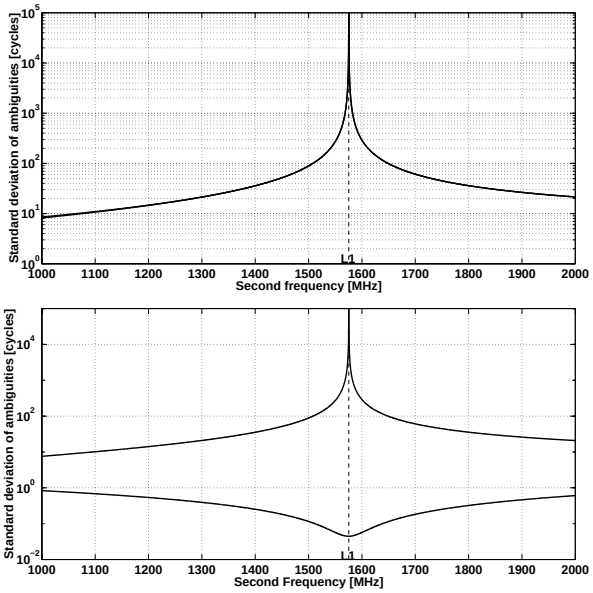

Figure 3-2: The single epoch, ionosphere float, dual-frequency, ambiguity standard deviations (cycles) as function of the second frequency (MHz). The top graph shows the precision of the two DD ambiguities, while the lower graph shows the precision of the two LAMBDA transformed ambiguities.

3.2 Triple-frequency analysis

We will now continue with the triple-frequency analysis. Figure 3-3 shows the single epoch, ionosphere float, triple frequency, ambiguity success rate as function of a varying third frequency. The first two frequencies were fixed at the GPS L1 and L2 values.

When compared to figure 3-1, the figure shows that the addition of a third frequency indeed improves the success rate. The maximum value is a factor of about 10 larger. The success rates however, are still too small for single epoch ambiguity resolution to be successful.

This shows that instantaneous ambiguity resolution, when based on the geometry-free model, will remain impossible for long ranges, even when a third frequency is included.

Note that the success rate obtains its smallest values when the third frequency is identical to either the L1 or the L2 frequency. These two minima are however not equal to zero as is the case when only two frequencies are used. Since not all three frequencies are identical at these two minima, the ionospheric delays can still be estimated. As a result, the success rate does not drop to zero. Also note that the two minima are of the same order as the dual-frequency success rates. Finally note, as was the case with two frequencies, that improved ambiguity resolution performance is achieved if the third frequency is located as far away as possible from the two other frequencies.

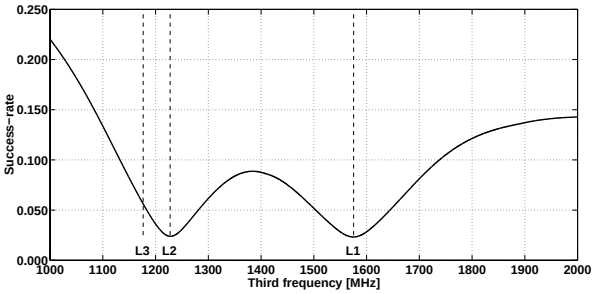

Figure 3-3: The single epoch, ionosphere-float, triple-frequency ambiguity success rate as function of the third frequency. The first two frequencies are fixed at the GPS L1 and L2 values. The dashed vertical lines indicate the current L1- and L2-frequency, as well as the chosen third GPS frequency.

In order to *explain* the signature of the success rate curve of figure 3-3, we will now consider the precision with which the ambiguities can be estimated. As was explained in the previous section, information on the standard deviations of the DD ambiguities is generally not sufficient to diagnose whether or not ambiguity resolution will be successful. Due to the decorrelation process applied, the precision curves of the *transformed* ambiguities however do give an explanation for the typical shape of the success rate curve. These precision curves are shown in figure 3-4. The lower graph of figure 3-4 shows the precision curves of the three transformed ambiguities. Two of these ambiguities are shown to have a (relatively) high precision, while the third ambiguity has a very poor precision. It is therefore the signature of this third precision curve which dominates the shape of the triple-frequency ambiguity success rate. Compare figure 3-4 with 3-3.

The minima and maxima of the three precision curves in the lower graph can be explained as follows. When $f_3=f_1$, the difference between the third and first DD ambiguity can be determined very precisely from the carrier phase data as $a_{31}=\phi_{31}/\lambda_1$. Similarly, when $f_3=f_2$ and a_{31} is known, the difference between the second and first DD ambiguity can be determined very precisely from the carrier phase data as $a_{21}=\phi_{32}/\lambda_2$. This explains the two minima in the two lower precision curves of figure 3-4. However, in either case $f_3=f_1$ or $f_3=f_2$, no phase-only solution exists for the first DD ambiguity when both a_{31} and a_{21} are known. This explains the two maxima of the third precision curve. In this case it is the poor precision of the code data that dominates the standard deviation.

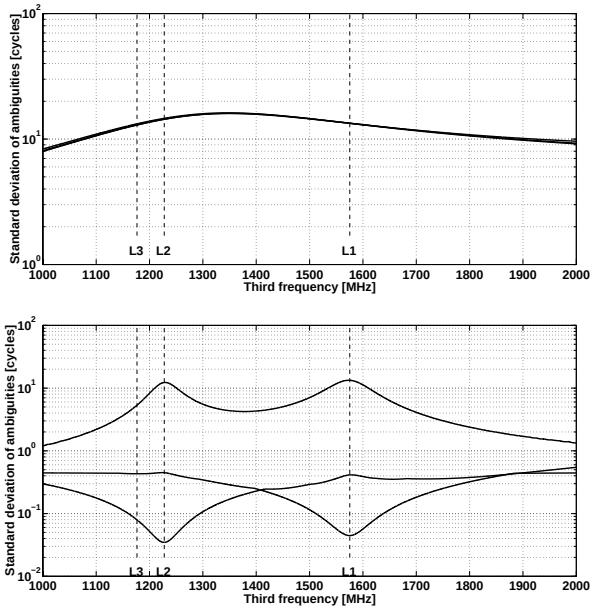

Figure 3-4: The single epoch, ionosphere float, triple-frequency, ambiguity standard deviations (cycles) as function of the third frequency (MHz). The top graph shows the (almost coinciding) precision of the three DD ambiguities, while the lower graph shows the precision of the three LAMBDA transformed ambiguities.

4. MORE EPOCHS AND BETTER PRECISION

So far the triple-frequency results were presented for a single epoch and for a fixed set of measurement precision values. In this final section we will show how the triple-frequency success rates change when some of these assumptions are changed.

Figure 4-1 shows the triple-frequency success rate curves for three different values of the undifferenced pseudo range standard deviations. As the figure shows, the success rates get larger when the pseudo range precision improves. These improvements however, are still far away from what is needed for instantaneous ambiguity resolution to be successful.

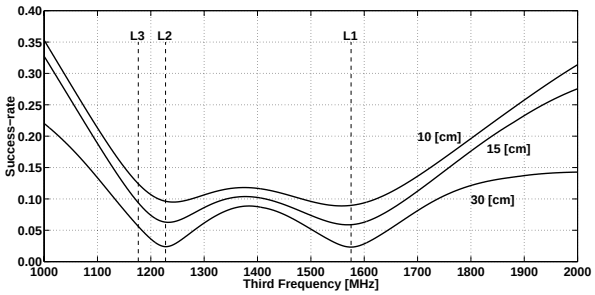

Figure 4-1: Single epoch, ionosphere-float, triple-frequency success rates for undifferenced pseudo range (code) standard deviations of 10, 15 and 30 cm and a fixed undifferenced carrier phase standard deviation of 3 mm.

Figure 4-2 again shows three triple-frequency success rate curves for the same pseudo range standard deviations as above, but now for an undifferenced carrier phase standard deviation fixed in cycles, namely 0.014 cycles. This implies, when expressed in range rather than cycles, that the carrier phase standard deviations will become dependent on the frequencies. Although this difference can be seen when comparing figures 4-1 and 4-2, it does not affect the conclusion that successful instantaneous long range ambiguity resolution is problematic.

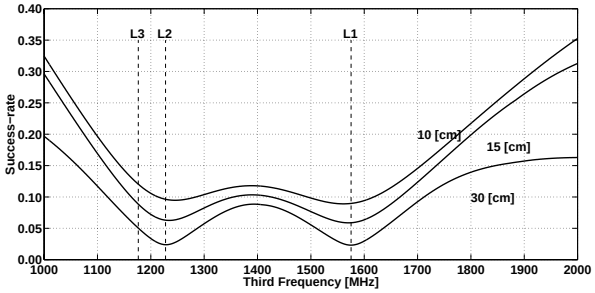

Figure 4-2: Single epoch, ionosphere-float, triple-frequency success rates for undifferenced pseudo range (code) standard deviations of 10, 15 and 30 cm and undifferenced carrier phase standard deviations of 0.014 cycles.

Knowing that geometry-free, instantaneous long range ambiguity resolution remains problematic, even when using three frequencies, it is of interest to know how many epochs are required to push the success rate sufficiently close to the ideal value of one. This is shown in figure 4-3. This result shows that quite some epochs are needed in order to get sufficiently high success rates. For the chosen three frequencies of modernized GPS this boils down to respectively 310, 440 or 760 epochs needed to obtain success rates of 90%, 95% or 99%.

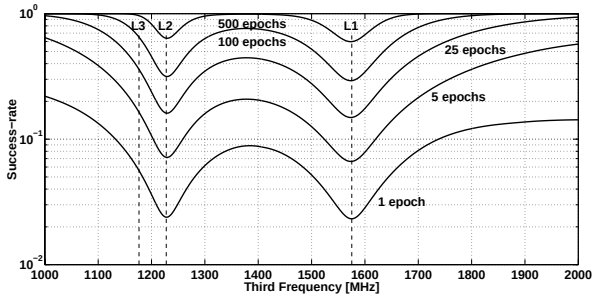

Figure 4-3: Ionosphere-float, triple-frequency success rates for some different number of epochs. The undifferenced pseudo range (code) and carrier phase standard deviations were set at 30 cm and 3 mm.

Although all our triple-frequency results were presented with two of the frequencies fixed at the current GPS L1- and L2-frequencies, the results also shed light on the expected performance of the proposed Galileo system. In the Galileo (GNSS-2) frequency scheme, one of the frequencies is located near the GPS L2 frequency, while the two other frequencies are both located very close to the GPS L1 frequency. This fact combined with the observation that frequency separation plays such a dominant role in ambiguity resolution, leads to the conclusion that the geometry-free, ambiguity success rates of Galileo will be smaller than those of the modernized GPS. This conclusion only holds true of course under the assumption that all design parameters, other than the three frequencies, are set at the same values for both Galileo and the modernized GPS.

Acknowledgement

N.F. Jonkman receives financial support from the Survey Department of the Dutch Ministry of Transport, Civil Works and Water Management.

5. REFERENCES

Ericson, S. (1999): A study of linear phase combinations in considering future civil GPS frequencies In: Proceedings ION GPS NTM-99, pp. 677-686.

Euler, H.J., C.C. Goad (1990): On optimal filtering of GPS dual-frequency observations without using orbit information. *Bulletin Geodesique*, Vol. 65, pp. 130-143.

Forsell, B., Martin-Neira, R.A. Harris (1997): Carrier phase ambiguity resolution in GNSS-2. In: Proceedings ION GPS-97, pp. 1727-1736.

Han, S., C. Rizos (1999): The impact of two additional civilian GPS frequencies on ambiguity resolution strategies. In: Proceedings 55th ION Annual Meeting, pp. 315-321.

Hatch, R. (1982): The synergism of GPS code and carrier phase measurements. In: Proceedings 3rd International Geodetic Symposium on Satellite Positioning, Vol. 2, pp. 1213-1231.

Hatch, R. (1996): The promise of a third frequency. *GPS World*, May 1996, pp. 55-58.

Hofmann-Wellenhof, B., H. Lichtenegger, J. Collins (1997): *Global Positioning System: Theory and Practice*. 4th edition. Springer Verlag.

Jonge de P.J., C.C.J.M. Tiberius (1996): The LAMBDA method for integer ambiguity estimation: implementation aspects. Delft Geodetic Computing Centre *LGR Series* No. 12, Delft University of Technology.

Jonkman, N.F., P.J.G. Teunissen, P. Joosten, D, Odijk (1999): GNSS long baseline ambiguity resolution: impact of a third navigation frequency. Accepted for publication in IAG proceedings of IUGG 22nd general assembly, 19-30 July, 1999, Birmingham, UK.

Joosten, P., P.J.G. Teunissen, N.F. Jonkman (1999): GNSS three carrier phase ambiguity resolution using the LAMBDA method. In: Proceedings GNSS'99, 3rd European Symposium on Global Navigation Satellite Systems, 5-8 October, 1999, Genova, Italy, pp. 367-372.

Strang G., K. Borre (1997): *Linear Algebra, Geodesy, and GPS*. Wellesley-Cambridge Press.

Teunissen, P.J.G. (1993): Least-squares estimation of the integer GPS ambiguities. Invited Lecture, Section IV Theory and Methodology, IAG General Meeting, Beijing, China. Also in: Delft Geodetic Computing Centre *LGR Series* No. 6, Delft University of Technology.

Teunissen, P.J.G. (1998a): The mean and the variance matrix of the 'fixed' GPS baseline. *Acta Geodaetica et Geophysica Hungarica*, Vol. 34 (1-2), pp. 33-40.

Teunissen, P.J.G. (1998b): A class of unbiased integer GPS ambiguity estimators. *Artificial Satellites*, Vol. 33, No. 1, pp 3-10.

Teunissen, P.J.G. (1998c): The distribution of the GPS baseline in case of integer least-squares estimation. *Artificial Satellites*, Vol. 33, No. 2, pp. 65-75.

Teunissen, P.J.G. (1998d): Success probability of integer GPS ambiguity rounding and bootstrapping. *Journal of Geodesy*, Vol. 72, pp. 606-612.

Teunissen, P.J.G. (1999): A theorem on maximizing the probability of correct integer estimation. *Artificial Satellites*, Vol. 34, No. 1, pp. 3-9.

Teunissen P.J.G., A. Kleusberg (eds) (1998): *GPS for Geodesy*, 2nd enlarged edition, Springer Heidelberg New York.

Teunissen, P.J.G., C.D. de Jong , (1999): Predicting the success of ambiguity resolution. Presented at CGSIC 34th meeting, September 12-14, 1999, Nashville, USA.
Available at http://www.navcen.uscg.mil/cgsic/meetings/summaryrpts/Default.htm.

Vollath, U., S. Birnbach, H. Landau (1998): Analysis of three-carrier ambiguity resolution (TCAR) technique for precise relative positioning in GNSS-2. In: Proceedings ION GPS-98, pp. 417-426.